Contribution of Tidal Power Generation System for Damping Inter-area Oscillation

S. Mehri[a], M. Shafie-khah[b,c], P. Siano[b], M. Moallem[a], M. Mokhtari[d], J.P.S. Catalão[c,e,f*]

[a] Department of Electrical and Computer Engineering, Isfahan University of Technology, Isfahan84156-83111, Iran
[b] University of Salerno, Via Giovanni Paolo II, 132, Fisciano (SA), 84084 Salerno, Italy
[c] C-MAST, University of Beira Interior, R. Fonte do Lameiro, 6201-001 Covilhã, Portugal
[d] Iran Grid Management Company (IGMC), Iran
[e] INESC TEC and Faculty of Engineering of the University of Porto, R. Dr. Roberto Frias, 4200-465 Porto, Portugal
[f] INESC-ID, Instituto Superior Técnico, University of Lisbon, Av. Rovisco Pais, 1, 1049-001 Lisbon, Portugal

Abstract

The growing need for the clean and renewable energy has led to the fast development of grid-connected tidal stream power generation systems all over the world. These large scale tidal stream power generation systems are going to be connected to power systems and one of the important subjects that should be investigated is its impacts on power system stability. Hence, this paper investigates the possibility of tidal stream power generation system on damping inter-area oscillations, as a new contribution to earlier studies. As tidal farms are mostly installed far from conventional power plants, local signals do not include good quality to alleviate inter-area oscillations. To overcome the problem, a novel damping controller is developed by employing wide-area measurement system and added to base controllers of doubly-fed induction generator through tidal stream power generation system. The proposed wide-area damping controller includes efficient means to compensate for the incompatible performances of wide area measurement based delayed signals. Robustness of the designed damping controller has been demonstrated by facing the study system with faults leading to enough shifts in power system operating point, and tidal farm generation.

Keywords: Wide-Area Damping Controller; Tidal Power Generation System; Power Oscillations; Teaching-Learning-Based-Optimization.

1. Introduction

As the renewable generators penetration continually increases in the power systems, it is of paramount importance to study the effect of these renewable generator integrated power systems on overall system stability. For example, application of Double Feed Induction Generator (DFIG) based wind farms in mitigating inter-area oscillations have been studied in the literature [1]. Or in [2] a novel approach for SSR mitigation with DFIG has been addressed.

Transmission voltage-level photovoltaic (PV) plants are another kind of renewable power plants that has been used for power system dynamic improvement.

* Corresponding Author at Faculty of Engineering of the University of Porto. E-mail address: catalao@ubi.pt (J.P.S. Catalão).

For example, recently R. Shah *et al*. [3] have proposed a mini max linear quadratic Gaussian-based damping controller for a large-scale PV plant to inter area oscillation damping or in [4] the impact of large-scale PV on rotor angle stability, particularly on inter-area oscillation is analysed as compared to the synchronous generator of same MVA rating at PV location.

In addition to the widespread installation of large-scale wind farms and PV plants, worldwide capacity of grid-connected tidal power generation system (TPGS) is growing rapidly [5]. There are two scenarios in which tides can be tapped for energy. The first is in changing sea levels. This phenomenon is responsible for the advancing and receding tides on shorelines. With the help of turbines, incoming tides can be manipulated to generate electricity. This scenario is called tidal barrage power generation system. The second way to exploit tidal energy is by sinking turbines to the sea floor. In this kind of TPGS fast-flowing currents turn generator blades much like the wind does with a wind turbine. This scenario is called tidal stream power generation system [6].

In the past, large-scale barrage systems dominated the tidal power scene. But because of increasingly evident unfavourable environmental and economic drawbacks with this technology, research into the field of tidal power shifted from barrage systems to tidal current turbines in the last few decades. This new technology leaves a smaller environmental footprint than tidal barrages.

Since turbines are placed in offshore currents avoiding the need to construct dams to capture the tides along ecologically fragile coastlines. Tidal stream generators draw energy from water currents in much the same way as wind turbines draw energy from air currents. However, the potential for power generation by an individual tidal turbine can be greater than that of similarly rated wind energy turbine. The higher density of water relative to air (water is about 800 times the density of air) means that a single generator can provide significant power at low tidal flow velocities compared with similar wind speed [7]. With growing installation of the DFIG based stream TPGS over the world, the question that arises is: Can the power converters used DFIG based stream TPGS be used to mitigate inter area oscillation? In this paper, such possibility is investigated.

The Grid Side Converter (GSC) of the DFIG may work such a shunt Flexible Ac Transmission Systems (FACTS) device. It can be used to voltage control like an STATCOM. STATCOM's ability to damping power swings has been demonstrated [8]. In [8] it has been shown that with including the auxiliary damping controller in the core control loop of STATCOM, inter-area oscillations are considerably damped. In this article, the GSC of the DFIG based TPGS is used like an STATCOM and it is utilized to damp inter-area oscillations.

Owing to the fact that FACTS and HVDC systems are usually installed on the critical points of the power system like important transmission lines or major generation plants, locally measured feedback signals can be used for the auxiliary damping controller of these devices. But owing to the fact that TPGSs usually located far away from critical points of power systems, it seems that locally measured feedback signals cannot be a good choice for DFIG based damping controller input signal. It is well known that, if wide area feedback signals are used on damping controller design, the damping controller operation can be improved unlike the local feedback signals [9].

Recent technological progress on WAMS, phasor measurement unit (PMU) and data communication technologies, allow the utility companies to use wide area signals for efficient mitigating the controller design. The achievements are mainly because of the time-stamped synchronous measurements that can be implemented in all areas of a geographically expanded power system [10].

The time which is demanded to communicate PMU data toward the system or regional control center plus that of transferring commands to control devices is totally considered as the communication delay or latency. The amount of the latency is dependent on the data transmission loading.

In wide area control systems, it reduces the impact of the control systems and can even completely destroy the control system behavior [10]. Therefore, considering this time delay through the controller design method is an important necessity and, a lot of studies have been reported to compensate destructive impacts of communication delay on wide area controller design [10]-[15]. In [10], a fuzzy logic Wide-Area Damping Controller (WADC) for inter-area oscillations damping and continuous latency compensation has been presented.

In [11], an adaptive phasor power oscillations damping controller has been proposed wherein the rotating coordinates were adjusted for continuous compensation of time-varying latencies. Reference [12] has investigated a linear control design technique that utilizes an optimization-based iterative algorithm with a set of linear matrix inequality constraints.

The method proposed in [13] is to obtain the optimal controller parameters, while efficiently considering the data transmission delay. In [14], a practical experience on the HVDC-based damping controller incorporating the communication time delay has been reported. In [15], a wide-area power system stabilizer for the small signal stability has been designed where a second order approximation has been considered for the sake of latency compensation.

The major contribution of this article is to demonstrate the applicability of DFIG-based marine farms in power system dynamic stability enhancement and mitigating of inter-area oscillations in the presence of WAMS technology. To the best knowledge of the authors, employing tidal power plants to alleviate the inter-area oscillations has not been addressed. Using high penetration of DFIG based wind farms as an effective solution for inter-area oscillations mitigation has been widely reported in the literature [1]. But the application of large scale TPGSs for alleviating inter-area oscillations has not been investigated. The main difference between wind DFIG ant tidal stream DFIG is their turbine mover fluid and their speed deviations. In most of the previous papers, the application of wind DFIG in oscillation damping has been studied so that the wind speed sticks at a constant amount during the simulation period [1]-[2]. However, in the current paper, it is assumed that the marine current speed is not constant and varies to lower than nominal marine speed.

The proposed WADC is a double stage conventional damping controller adjusted by Teaching-Learning-Based-Optimization (TLBO) method for inter-area oscillations mitigation and continuous coverage of time-varying delay. The suggested structure is added to a standard multi-machine power system and comprehensive nonlinear simulations are used to execute the useful performance of the suggested structure. Also, the robustness of the proposed damping controller is examined through various case studies.

The rest of the paper is organized as follows. In Section 2, the effect of the fault duration change and system reconfiguration is examined on the performance of the suggested damping controller in mitigating fluctuations. In Section 3, simulation results are carried out in two values for marine current speed and tidal farm output active power, to assess the effectiveness of the suggested structure when the marine current speed and accordingly tidal farm active power delivered to the system varies to a lower value. Finally, Section 4 concludes the paper.

2. Material and Methods

2.1. Marine current Speed and Marine Turbine

The global scheme for a practical DFIG based tidal stream power generation system is given by Fig. 1. In the following, the detailed models for all sections of a TPGS are introduced.

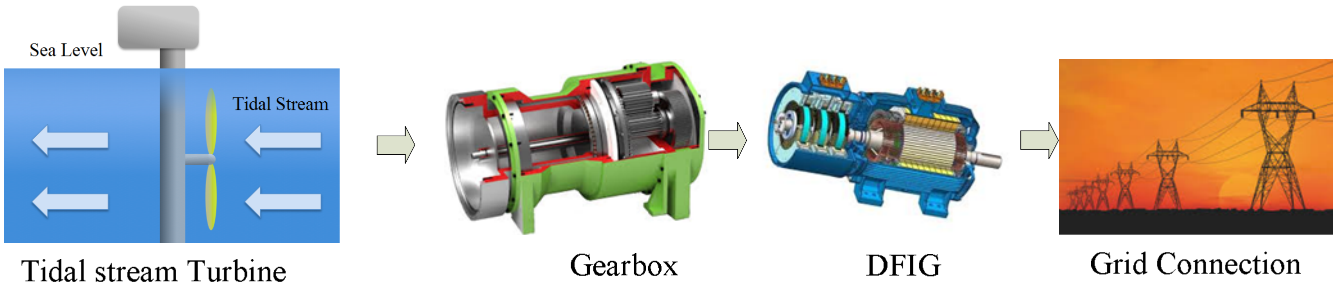

Fig. 1. The global scheme for a practical DFIG based tidal stream power generation system

Tidal stream generators draw energy from water currents similar to the way that wind turbines draw energy from air currents. Ordinary the tide speeds (i.e., spring and neap tides) move the Marine Current Turbine (MCT) [5]. Some shorelines experience a semi-diurnal tide, two nearly equal high and low tides each day. Other locations experience a diurnal tide, only one high and low tide each day. A "mixed tide"; two uneven tides a day, or one high and one low, is also possible. The marine-currents are determined to start at 6 hours before high waters and to end 6 hours after them. On this basis, deriving a simple and applied plan is not difficult for marine-current speeds, since tide factors can be obtained as follows:

$$V_{MR} = V_{nt} + \frac{(C_{mr} - 45)(V_{st} - V_{nt})}{95 - 45} \quad (1)$$

Where V_{MR} denotes the marine speed in m/s.C_{mr} represents the marine factor, 95 and 45 denote the average factors of spring and neap tides, respectively.V_{st} and V_{nt}respectively represent the marine-current speed of the spring and neap tides (for the area between France and England) [16]. The mechanical power of the considered MCT is illustrated in Equation (2).

$$P_{mmr} = \frac{1}{2}\rho_{mr}.A_{rmr}.V_{MR}^{3}.C_{pmr}.(\lambda_{mr},\beta_{mr}) \quad (2)$$

Where $\rho_{mr} = 1025$ kg/m denotes the seawater density, A_{rmr} represents the blade impact area in m^2, and C_{pmr} denotes the power coefficient C_{pmr} of the MCT is given by

$$C_{pmr}(\psi_{mr},\beta_{mr}) = d_1\left(\frac{d_2}{\psi_{mr}} - d_3.\beta_{mr} - d_4.\beta_{mr}^{d_5} - d_6\right)exp\left(-\frac{d_7}{\psi_{mr}}\right) \quad (3)$$

in which

$$\frac{1}{\psi_{mr}} = \frac{1}{\lambda_{mr} + d_8\,.\beta_{mr}} - \frac{d_9}{\beta_{mr}^{3} + 1} \quad (4)$$

$$\lambda_{mr} = \frac{R_{bmr} \cdot \omega_{bmr}}{V_{MR}} \tag{5}$$

where ω_{bmr} is the blade angular velocity (rad/s), R_{bmr} is the blade radius (m), λ_{mr} is the tip speed ratio, β_{mr} is the blade pitch angle (degrees), and $d_1 - d_9$ are the constant coefficients of power coefficient C_{pmr} of the MCT. Cut-in, rate, and cut-out speeds of MCT are considered 1, 2.5, and 4 m/s, respectively. For the times that V_{MR} are more than the nominal speed, the pitch-angle control loop starts decreasing the power of the MCT to the nominal one. Most of the mathematical formulations used in an offshore wind farm can be employed in the marine current farm, because the pitch-angle control loop, studied turbine, and mass-spring-damper models match with ones that are used in offshore wind farm [17].

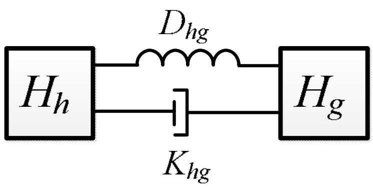

Fig. 2. The considered two-inertia reduced-order tantamount mass-spring-damper.

The two-inertia reduced-order equivalent mass-spring damper model of the wind turbine directly coupled to the rotor shaft of the wind DFIG is shown in Fig. 2 [18]. This model can also be applied to the equivalent mass-spring-damper model of the marine current turbine coupled to the rotor shaft of the marine-current DFIG through an equivalent gearbox (GB) whose effect can be properly included in this model. The equations of motion for the two-inertia reduced-order marine current turbine model shown in Fig. 2 are expressed by [18]-[19].

$$(2H_{ht})p(\omega ht) = T_{tm} - K_{hg}\theta_{hgt} - D_{hg}\omega_{ht} \tag{6}$$

$$(2H_{gt})p(\omega_{gt}) = K_{hg}\theta_{hgt} + D_{hg}\omega_{gt} - T_{eg} \tag{7}$$

$$p(\theta_{hgt}) = \omega_b(\omega_{ht} - \omega_{gt}) \tag{8}$$

where ω_b denotes the base angular speed. H_{ht} and H_{gt} represent inertias of tidal turbine and DFIG, respectively.K_{hg} and D_{hg} denote the stiffness and damping coefficients between tidal turbine and DFIG, respectively. ω and θ represent the angular speed and angle movement of each mass, respectively. T_{eg} denotes electromagnetic torque [19].

2.2. *Tidal DFIG*

In terms of the system topology, tidal turbine generators can be classified into five groups as illustrated in Fig. 3[7]. Compared to a fixed-speed marine generator, the most important benefits of the variable-speed generator are:

1) The capability of variable-speed generators on extracting maximum energy at different tidal flows through rotor speed regulation.

2) Decrease mechanical pressure inflicts on the turbine. Moreover, the fixed-speed generators preserve a fixed rotor speed. Albeit it needs ordinary power electronic equipment, the fixed-speed induction generators do not have a high effectiveness of tidal power conversion and the capability to make voltage and reactive power control. In addition, it enforces tense mechanical stresses on the turbines and needs a more complicated pitch control to preserve a fixed rotor speed [7].

DFIG is an improved form of a usual induction generator so that it uses a series voltage source converter namely rotor-side converter (RSC) to supply the wound rotor. It also consists of a grid-side converter (GSC) to supply reactive powers and voltage controls of DFIG. Controllability of this converters is the main advantage of DFIG over other wind and tidal generation systems [7].

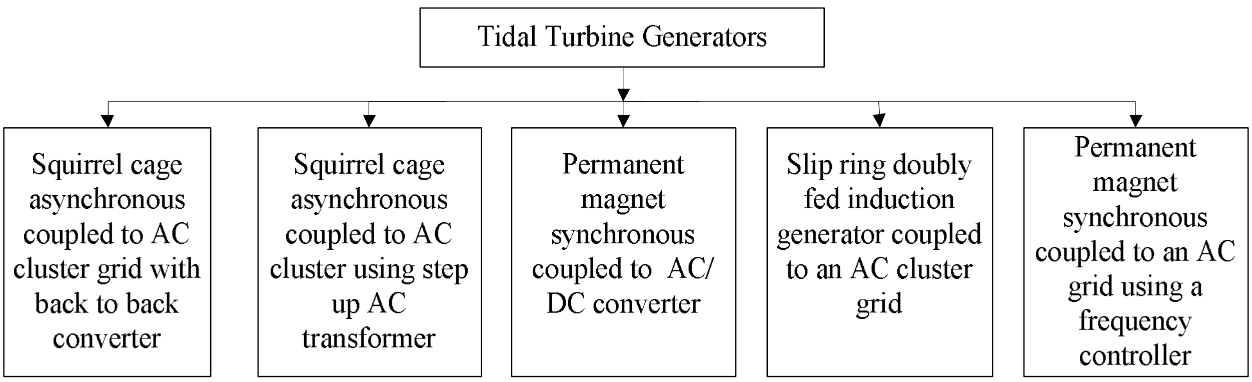

Fig. 3. Classification of tidal turbine generators [7].

The two main control systems of TPGSs are turbine and the converters' control. The main task of tidal turbine control is the controlling speed of the tidal turbine and system frequency through variable marine current speeds as well as the optimizing of power production. The main task of converters control is controlling the DFIGs produced active and reactive power. Fig. 4 (a) indicates the control framework of RSC. The q axis loop is employed to adjust the DFIG's active power (i.e., P), whereas the d axis loop is used to adjust the reactive power (i.e., Q). The conventional PI controllers can be utilized for regulation of P and Q. Also Fig. 4 (b) illustrates the control structure of the GSC. The GSC aims at maintaining DC-link voltage fixed with ignoring the value and side of the rotor power and controlling the voltage and reactive power of DFIG GSC (Qg). Likewise, the generic PI controllers are employed as a controller in both DC voltage and Qg control loops. In order to alleviate inter-area oscillations, auxiliary damping controllers can be added to RSC and GSC control loops.

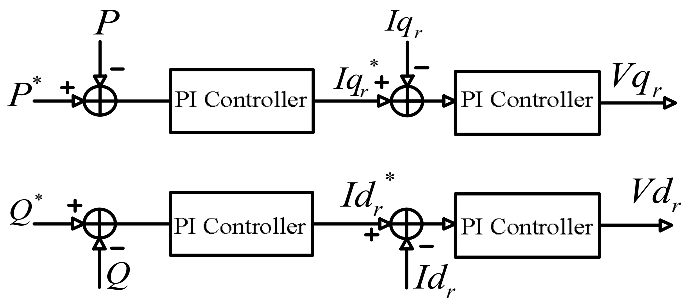

(a)

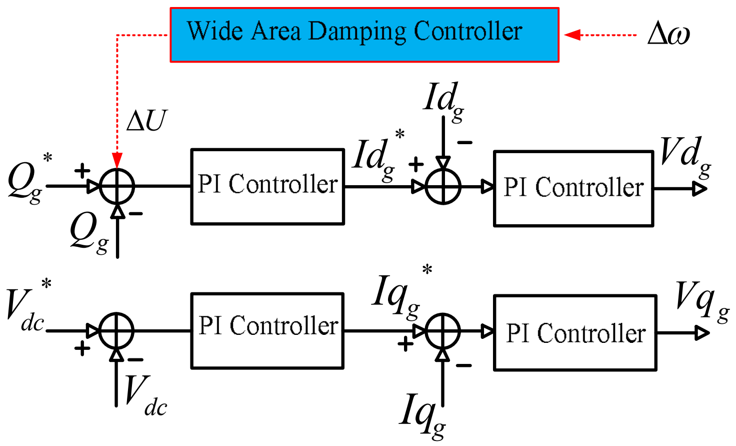

(b)

Fig. 4. (a) Control structure of DFIG's RSC, (b) Control structure of DFIG's GSC

2.3. Teaching-learning-based optimization algorithm

One of the most newly developed metaheuristic methods is TLBO [20]-[21]. TLBO has some inherent capabilities and advantages compared to other metaheuristic approaches. One of the important problems of whole evolutionary and swarm based methods is this subject that they need controlling parameters, e.g., the population and the generations' number. Furthermore, typical control parameters, various methods need the particular algorithm-specific control parameters. For instance, GA utilizes mutation and crossover rates. Or, PSO employs inertia weight and social and perceptive parameters. The suitable adjusting of these parameters is, indeed, one of the most important problems of evolutionary and swarm based methods. But unlike the mentioned algorithms, TLBO needs no algorithm-specific parameters [20].This is one of the main benefits of TLBO compared to other metaheuristic approaches because common control parameters are joint in solving each population-based optimization methods; algorithm-specific parameters are particular to that method and various methods have various particular parameters to control. TLBO has many similarities to evolutionary algorithms (EAs): an initial population is randomly selected, moving on the way to the teacher and classmates is comparable to mutation operator in EA, and selection is based on comparing two solutions in which the better one always survives [22].

TLBO is an optimization method on the basis of learning procedure in a classroom. The searching procedure contains two stages, namely, *Teacher Phase* and *Learner Phase*. Primarily, students achieve learning from a teacher. Afterward, they learn from classmates. The finest solution of the whole population is assumed as the teacher ($X_{teacher}$).

In other words, in the first stage that is teacher phase, students receive knowledge from the teacher. In the stage, the teacher attempts to raise the outcomes of persons (X_i) by raising the average outcomes of the classroom (X_{mean}) to its outcome $X_{teacher}$. For keeping stochastic characterizes of the search, two random factors (i.e., r and T_F) are utilized to renew the outcome X_i as:

$$X_{new} = X_i + r.(X_{teacher} - T_F.X_{mean}) \tag{10}$$

where r denotes a random amount between 0 and 1. T_F represents the teaching factor (either 1 or 2):

$$T_F^i = round[1 + rand(0,1)\{2-1\}] \tag{11}$$

It is considerable that, X_{new} and X_i denote the new and available solution of i, [20]. In the learner stage, the students try to enhance their writing by collaboration with other students. So, an individual can learn new knowledge if its knowledge is less than the others. All over this stage, the learner X_i accidentally cooperates with another learner X_j ($i \neq j$) to enhance its learning. When X_j has finer solution than X_i, X_i will move toward X_j, otherwise, it will move away:

$$X_{new} = \begin{cases} X_i + r.\left(X_j - X_i\right), & f(X_i) > f\left(X_j\right) \\ X_i + r.\left(X_i - X_j\right), & f(X_i) < f\left(X_j\right) \end{cases} \tag{12}$$

If the new outcome (i.e., X_{new}) is finer, the population will accept it. The algorithm continues until the termination conditions are met. The flowchart of the proposed TLBO algorithm is shown in Fig. 5 and the pseudo code presented in Appendix (Table A1) demonstrates the TLBO algorithm step-by-step [22].

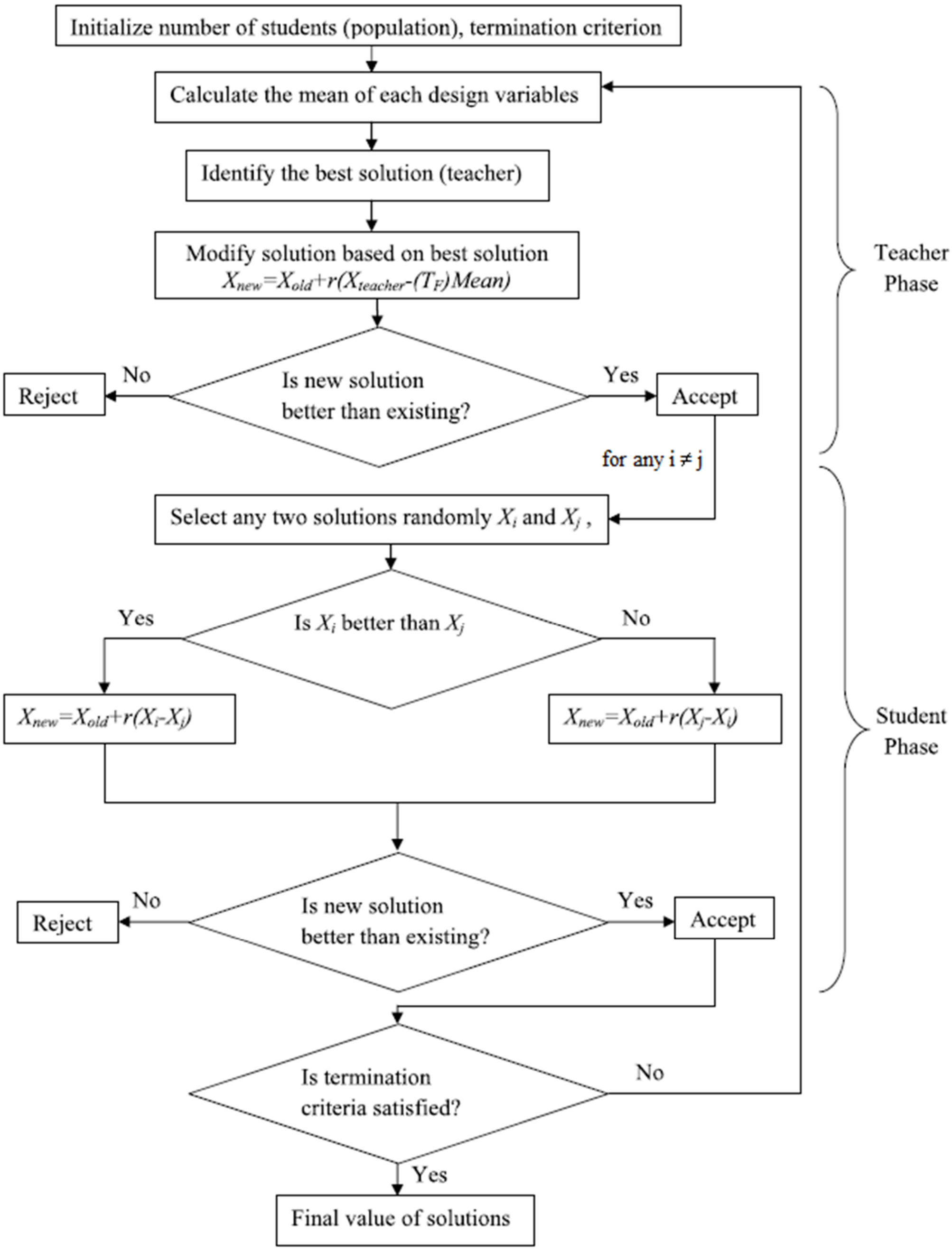

Fig. 5. Flowchart of the proposed TLBO algorithm

3. Results and Discussion

3.1. The Studied Power System

Because the main purpose of this paper is about damping of inter area fluctuations, the system chosen for case study must be a large power system with multiple machines and several areas. So, in this paper the well-known three area - six machine power system is used in this section as an example to validate the performance of the proposed structure on inter area oscillation damping. The single-line diagram of the network is shown in Fig. 6. The system has six synchronous generators rated at 900 MVA each with identical controls, distributed in three generation and load areas interconnected by transmission lines. Each area has two generators and each one is delivering around 700MW. The detailed parameters of the three area six machine power system is shown in Appendix (Table A2 and A3).

To show the ability of DFIG based Tidal stream farm in inter area oscillation damping, a high penetration DFIG based Tidal stream form is installed to the bus 7 by a 100 km transmission line. The rated power of stream tidal farm is assumed to be 202.5 MW (integration of 135 stream turbines with the rated power of 1.5 MW). A tantamount single DFIG is assumed to show the aggregative performance of the set of the tidal turbines. This assumption is practicable and in most articles published in the field, this technique has been used [1]-[2]. In these papers, it was shown that for the power system dynamic studies, a high penetration single DFIG Offers acceptable performance. Since for an aggregated high penetration individual DFIG, the integrated inertia, and the base power are scaled up, per unit amount of parameters is fixed. Therefore, per unit amount of a high penetration individual DFIG based TPGS is equal with per unit values of a 1.5 MW DFIG based TPGS. The parameters of a single 1.5MW DFIG and the equivalent marine farm are listed in Appendix (Table A4). The detailed information and characteristics of the tidal farm are taken from [1].

By the use of eigenvalue method, it was found that the 6 machine 3 area power systems have two separate inter-area modes with frequency of 0.78 and 0.46 Hz. The 78 Hz mode is the inter-area mode with G1 and G2 swinging versus G5 and G6 and also the 0.46 Hz mode includes generators of area 2 swings versus the ones of area 1 and area 3 [10]. Therefore, due to these oscillatory modes, it seems that it is necessary to design an appropriate damping controller for damping an unsteady oscillation mode. A TLBO-based WADC is developed and supplemented to the conventional control framework of the DFIG based marine farm.

3.2. Damping Controller based on Wide Area Monitoring System

The use of PMUs is growing around the world due to its large extent applications. Opposite to the conventional measurement devices, PMUs are synchronized respect to each other through the one pulse per second signals of the global positioning system. This new opportunity realized the true concept of measuring phase angles which inherently encompass valuable information of the system stress situation.

A WAMS is required to gather the PMUs' data which is sent from designated places in the power system and stored in a data storage system each 100 milliseconds.

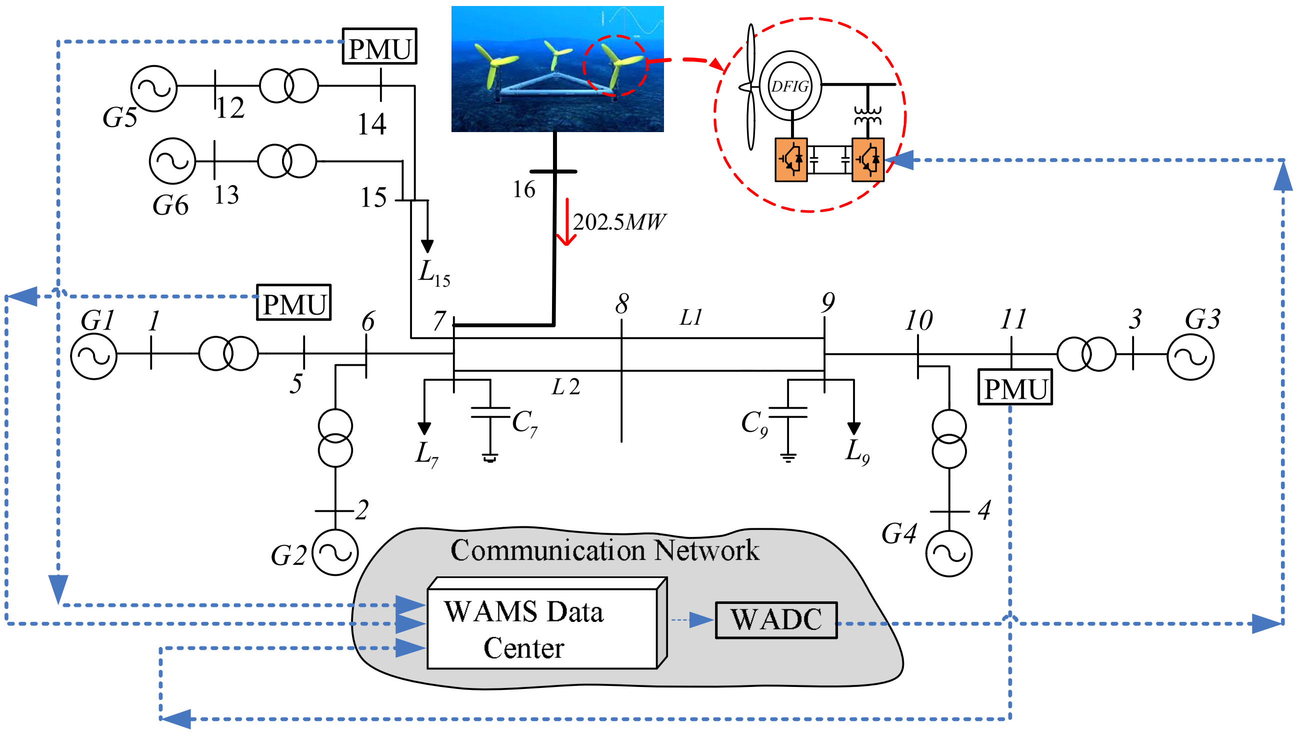

Fig. 6. The considered power system with a DFIG marine farm.

One of the most practical applications of WAMS is oscillation damping which highly depends on the number and location of PMUs placed on the grid. In order to oscillation damping, it seems that a definite number of PMUs will meet the objective where the places of PMUs are chosen properly. This claim is proved by the numerical studies provided in the following. The mentioned issue is intended by the authors for future work whereas some pioneering research is currently available [23].

A local damping controller is not indeed able to access to the oscillation signals while wide-area modal keep being observable. On the contrary, WAMS application makes it possible to achieve global inter-area oscillation information to apply to the damping controller. The most important contributing factor in the efficient behavior of WADC is to feed the feedback signal delays to the controller; whereas, the local damping controller does not have this concern. Obviously, WADC and local controller structure design are basically different due to the difference of their input signals. WADC can alleviate multi-mode fluctuations. This capability is indicated by multi-band controllers which each exerts its own global input signal to damp one of the oscillation modes. But, local damping controllers have only one band to alleviate an oscillation mode.

Since the considered system includes two inter-area modes, a two-band controller is employed as illustrated in Fig. 7. Band controllers are denoted by WADC1 and WADC2 and the whole unit is recognized by WADC.

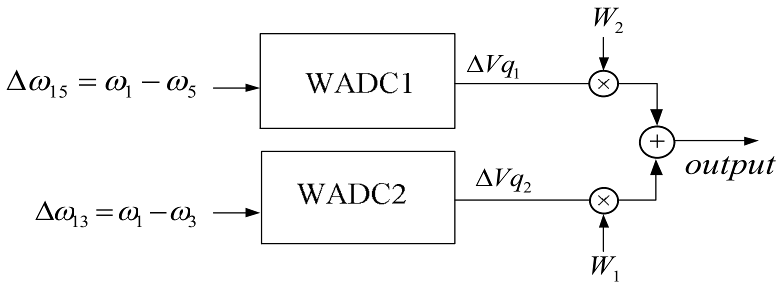

Fig. 7. The considered two-band WADC.

Apparently, to alleviate multi-mode oscillations, it is essential to have two additional signals including both modes of oscillation. Any type of input signals which has suitable modal observability of inter-area oscillations may be utilized, e.g., the tie line power, the frequency difference of areas, and angle difference of areas.

Commonly, PMUs receive the three-phase voltage and current in a sinusoidal waveform. Afterward, the phasor values are obtained by converting the sampled digital data, and will be sent to the system control center.

Even though the PMU's frequency and the rate of change depend on measuring the voltage, a number of methods have been reported to compute the generator's speed via local PMU measurements [24]-[26].

Frequency indeed has a crucial role for the system stability and balance between generations and loads. Frequency (or rotor speed) and the rates of change can be employed as the damping controller feedback signal [1]-[2] and [10]. On this basis, it is assumed that PMUs located on high voltage buses (connected to G1, G3, and G5) where $\Delta\omega_{13}=\omega_1-\omega_3$ and $\Delta\omega_{15}=\omega_1-\omega_5$ are considered as global feedback signals. $\Delta\omega_{15}$ and $\Delta\omega_{13}$ are applied as the input of WADC1 and WADC2 respectively to alleviate the inter-area oscillation modes 1 (0.78 Hz) and 2 (0.46 Hz) correspondingly. As shown in Fig. 7, the output of WADC is weighted of both modes as indicated by equation (9).

$$output = W_1 \Delta Vq_1 + W_2 \Delta Vq_2 \tag{13}$$

where, W1 and W2 considered as weighting factors which obtained from the Prony analysis inversely proportional to normalize damping ratio of their main mode (W1=1.15, W2=1) [10]. The WADC output is lastly used for modulation of the DFIG's reactive power loop.

Time synchronized data gathering and sending by the time-stamped PMUs makes the communication latency computable if the local times of controller location are accessible through devoted GPS equipment.

The entire latency of transferred data can be computed by comparing the local time at the controller and the instant of origin at the PMUs' location [27]. It is necessary to note that if the controlled equipment is far from the controller, the transmitting time of the commands is also considered. Due to the uncertainty of the communication system, the latency does not get fixed completely.

To evaluate the effects of time delay, an ideal designed WADC is examined in this study where the feedback signal has several levels of time delay. As shown in Fig. 8, the total latency includes the sum of a fixed value and a random number, i.e., 300 ±rand(50) milliseconds where the time delay variable is applied randomly.

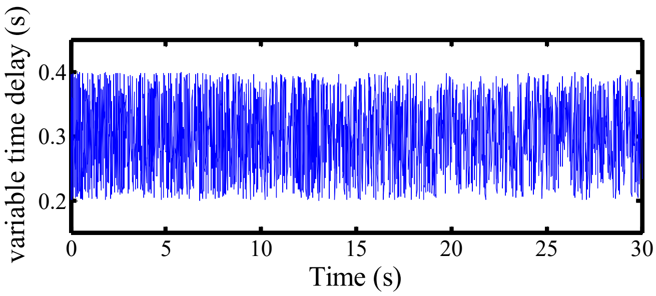

Fig. 8. Random time delay of the remote feedback signal.

Here the tendency is to design a WADC, called delay-compensated WADC, in order to compensate for the destructive effects resulted from the time delays. To meet this end, an additional input signal that represents the latency of feedback signal is required to feed the DFIGs location to the damping controller. The parameter of the time delay is implemented to the simulation setup throughout the design procedure and then the TLBO algorithm optimizes the controller parameters. In this method, parameters of lead-lag compensator are adjusted, hence the phase shifts between speed deviation and resulted electrical damping torque are compensated, and the adverse effects of latency are also lessened.

300 ± rand (100) ms latencies in remote feedback signals are taken into account to design the latency-compensated WADC. The final values of the WADC parameters are presented in Table I.

TABLE I
Parameters of Latency-Compensated WADCs

Type	***K***	T_W	T_1	T_2	T_3	T_4	**min & max**
WADC1	38	2	0.018	2	0.008	0.001	±0.1
WADC2	33	2	2.1	0.001	2	0.001	±0.1

To simulate a disturbance on the system, a three phase fault with duration of 50 ms is applied at t = 10 s near bus 8 to confirm the control operation of tidal DFIG based WADC. Fig. 9 displays the dynamic reaction of the study system where the disturbance is applied. It is obvious that in the case without WADC, there are unstable inter-area oscillations between three areas, which is obviously displayed by the rotor speed difference of G1 and G3, and G1 and G5 and the active power through tie-line 7–9 (shown in Fig. 9 a-c). In contrast, when the designed WADC is included in the core control loop of tidal DFIG, all sorts of oscillations are well damped and the tidal DFIG equipped with WADC can easily mitigate the inter-area oscillations with 300 ± rand (100) ms latency on remote feedback signals (shown in Fig. 9 a-c).

In Fig. 10 (a)-(b), reactive and active powers of the tidal DFIG are showed. It can be observed from Fig. 10 that the proposed tidal DFIG equipped with WADC can stabilize the system even with 300 ± rand (100) ms latency on remote feedback signals and the designed WADC can easily damp system oscillations. Also with considering 300 ± rand (100) ms latency on feedback signals, the designed WADC displays a good robustness against the time delay unpredictability and this feature of proposed WADC is of interest for real-world applications.

3.3. Sensitivity Analyses

This part is dedicated to examining the proposed WADC operation under various situations that the system can face with like tidal DFIG generated power changing and power system reconfiguration. The sensitivity analysis is accomplished to realized, the capability of the controller in tolerating the unfavourable conditions as well as the accuracy of its performance. It would be very useful for the designed WADC to preserve its operation suitable even in harsh situations.

Two different cases are examined to evaluate designed controller performance in oscillation mitigation. The cases considered here are as follows:

- Impact of the fault clearing time and system reconfiguration on oscillation damping
- Impact of changing marine current speed and tidal farm output power

In the following, various conditions that the system may be faced with, are simulated and the simulation outcomes are obtained for each condition exclusively and a comprehensive discussion is presented.

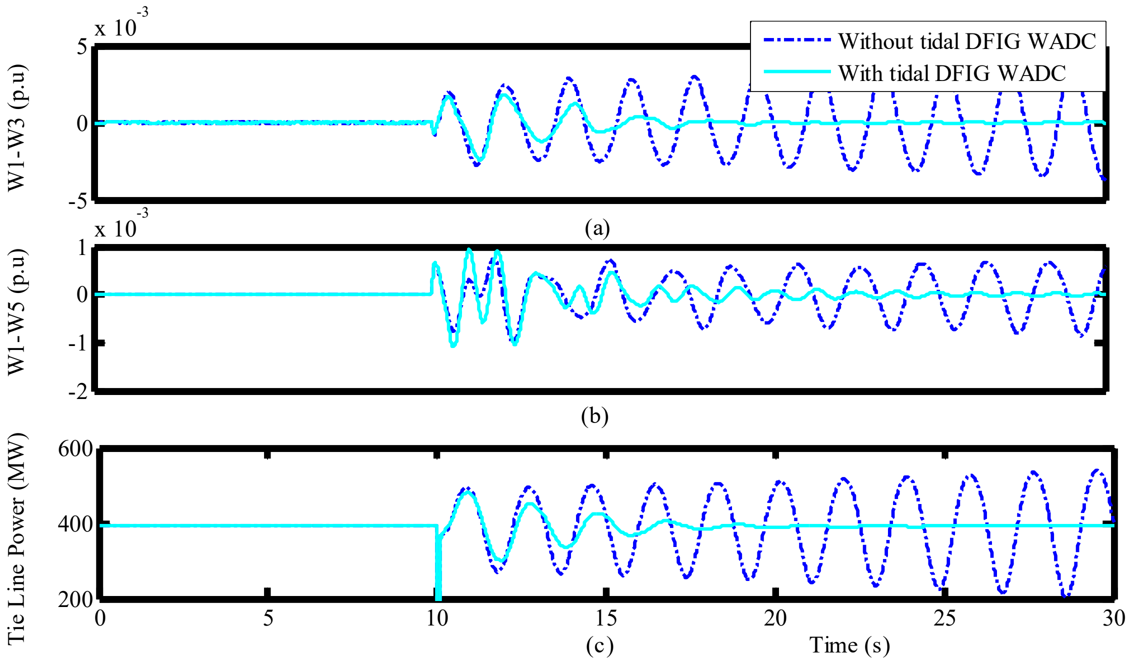

Fig. 9. Dynamic response to a fault at bus 8: (a) rotor speed difference of G1 and G3, (b) rotor speed difference of G1 and G5 and (c) power flow of tie-line 7–9.

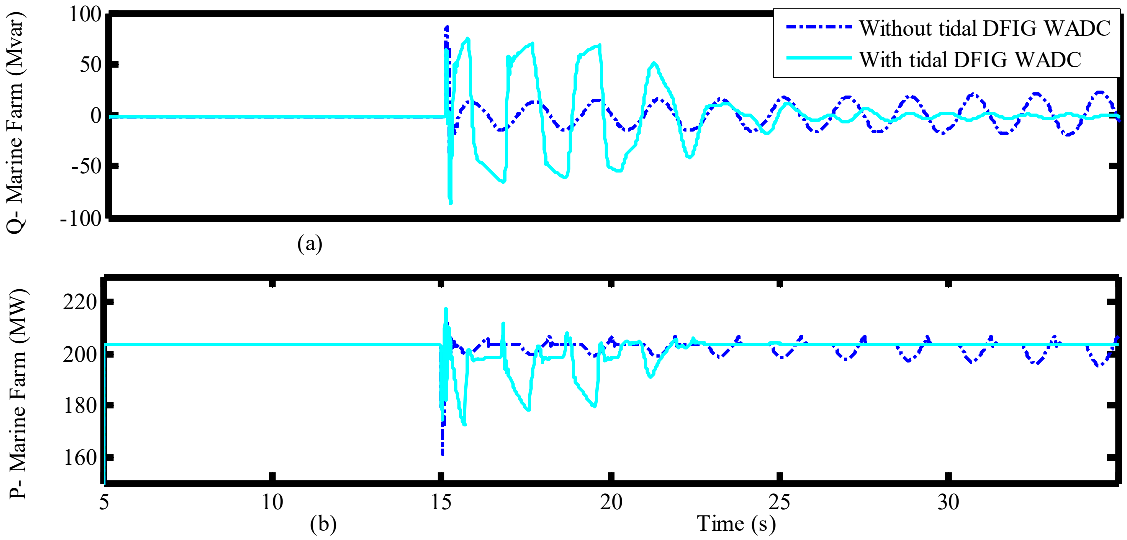

Fig. 10. Tidal turbine generation dynamic responses following a fault at bus 8 (a) DFIG reactive power, (b) DFIG active power.

3.3.1. Effect of the increasing Fault Clearing Time and power system reconfiguration on oscillation Damping

The impact of the system configuration on the success of the designed WADC in mitigating oscillations is investigated at a different system configuration. In this section in order to change the system configuration, the disturbance duration is increased to 0.15 sec at the line between buses7 and 8. It is also assumed that this fault duration is more than the system distance relays critical clearing time. As a result, after the occurrence of the fault, distance relay of the line between buses 7 and bus 8 responds to the fault with tripping this line. As a result of this action, the line between bus 7 and 8 is switched off from the system and the system configuration will be changed. Figure 11 (a) indicates the obtained rotor speed difference of G1 and G3, response to a fault with and without additional control. Similarly, Fig. 11 (b) illustrates the power flow of the tie-line 7–9. According to the simulation results that in such situation the system will be faced with very severe fluctuations but the additional control is also able to damp all sorts of oscillations arisen from a disturbance at a new system configuration.

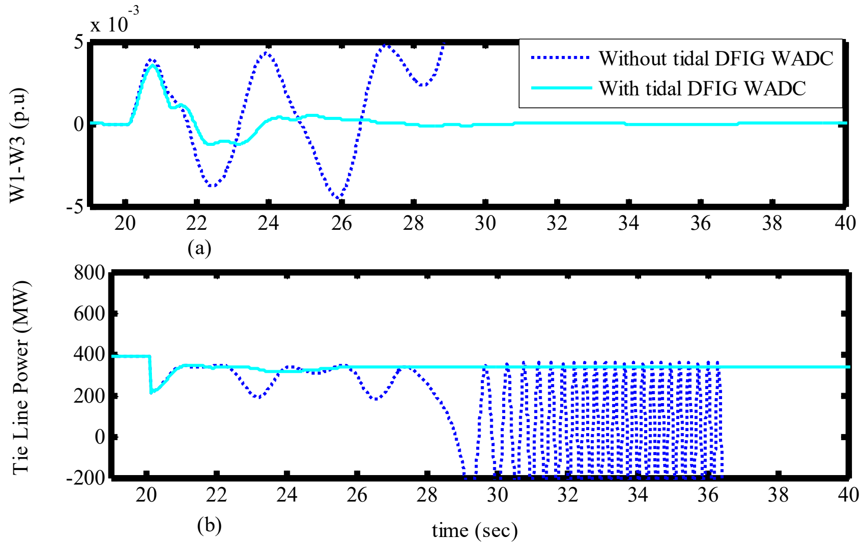

Fig. 11. Dynamic response to a fault at the line between bus 7 and 8 when the power system configuration is changed: (a) rotor speed difference of G1 and G3, (b) power flow of tie-line 7–9.

3.3.2. Effect of the increasing and decreasing of marine current speed and tidal farm generation

To evaluate the efficiency of the proposed structure when the marine current speed and accordingly tidal farm active power delivered to the system varies to a lower value, simulation results are carried out in two values for current speed and accordingly tidal output active power. At first, the marine current speed is set to its nominal value (3m/s) and consequently ideal farm active power will be set to 202.5 MW. At t=30 sec the marine current speed decreases to 1.6 (m/s) and as a result, the tidal farm active power decreases to 20 MW. Meanwhile, at t=40 sec a three-phase short-circuit fault with a duration of 50 ms occurs at bus 8. Fig. 12 (a) and (b) show the deviations of rotor speed of G1 and G3 and the DFIG rotor speed in pu, respectively. Also in Fig. 13 (a) and (b), reactive and active powers of the tidal DFIG are plotted. As it can be seen, the proposed structure successfully damps out the oscillations when the tidal farm active power varies to lower values.

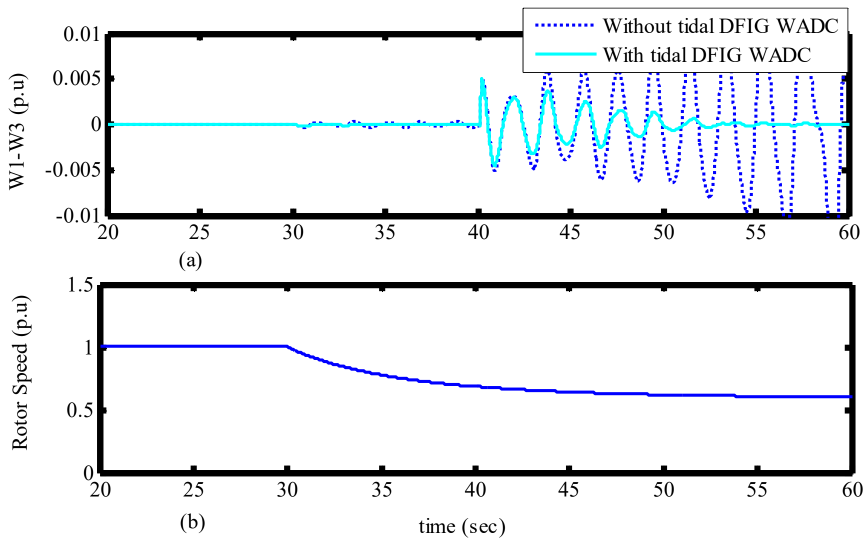

Fig. 12 Results of proposed WADC in oscillations attenuation when the tidal farm active power is changed: (a) rotor speed difference of G1 and G3, (b) rotor speed DFIG.

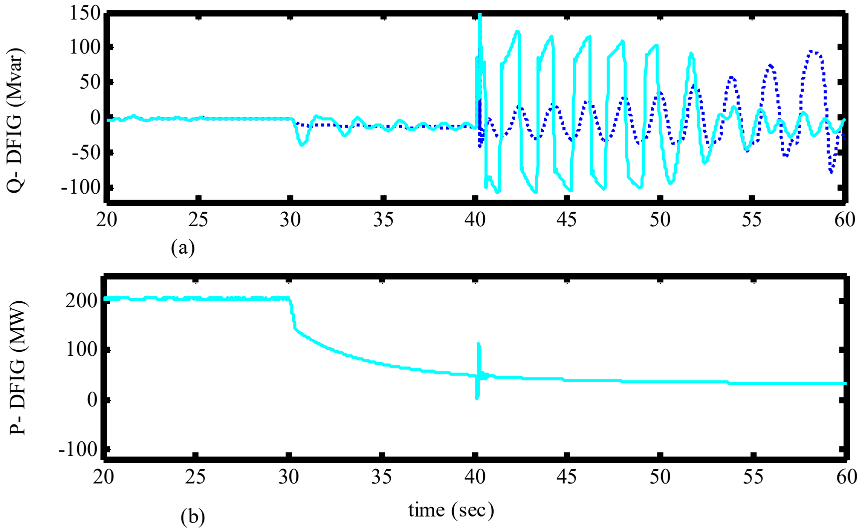

Fig. 13 Results of proposed WADC in oscillations attenuation when the tidal farm active power is changed: (a) reactive power of DFIG, (b) active power of DFIG.

4. Conclusions

This paper revealed the effectiveness of implementing a wide area measurement-based damping controller at a DFIG based tidal power plant to successfully alleviate the inter-area oscillations arisen from an interconnected power system. The oscillation damping was realized not by additional FACTS controller, but by adjusting the reactive power of the Tidal turbines own converter with a conventional two channel WADC. A vast body of literature is available on the utilizing FACTS controllers or DFIG based wind farms and PV farm as an effective solution for inter area oscillation damping. Mokhtari *et al* [1]-[2] have demonstrated the ability of DFIG based wind farm in mitigating SSR and inter area oscillation. In both references [1]-[2], a PSO based conventional damping controller has been designed and added to the main control loop of DFIG based wind farm to oscillation damping. Shah et all. [3] have shown that a high penetration PV plant can be utilized for inter area oscillations attenuation. There are many other manuscripts reporting the capability of all renewable power generation system for power system oscillation mitigation. However, to the best knowledge of the authors, this is the first work that shows the ability of DFIG based tidal stream farm to power system oscillation damping. Moreover, in all references cited above the renewable generation systems are assumed to have constant produced power, while in this work the tidal farm produced power changes are also considered in the simulation process. The Tidal farm auxiliary damping controllers implemented the variable areas generator rotor speed variations as a feedback signal to produce the auxiliary damping signal and the reactive power regulation of the DFIGs was utilized for inter-area fluctuations damping. The rotor speed deviations for damping controller were obtained through wide-area information due to the utilization of PMUs dispersed over the network. The TLBO approach was used for best adjusting of the controller's parameters and possible signal delay of feedback signals on WAMS was considered for the controller design. It was properly showed that the designed WADC operates suitably and displays excellent robustness against transmission time delay uncertainties. In addition, the obtained results with sensitivity analyses indicated that the operation of the designed WADC is highly robust against varying the fault duration time and power system operating point and tidal farm generation. With the rapidly increasing application of DFIG based tidal farms and PMUs, designing WAMS based supplementary control for tidal farms for power systems dynamic enhancement is necessary and needs many research activities. In this subject, the most important issue is the coordinated design of DFIGs and other renewable power generation systems like voltage-level PV plants based on using WAMS technology and considering the time-varying communication system delays. The subjects are open future research themes in the scope of renewable energy systems and smart transmission grids.

Acknowledgements

J.P.S. Catalão acknowledges FEDER funds through COMPETE 2020 and Portuguese funds through FCT, under Projects FCOMP-01-0124-FEDER-020282 (Ref. PTDC/EEA-EEL/118519/2010), POCI-01-0145-FEDER-016434, POCI-01-0145-FEDER-006961, UID/EEA/50014/2013, UID/CEC/50021/2013, and UID/EMS/00151/2013. Also, the research leading to these results has received funding from the EU Seventh Framework Programme FP7/2007-2013 under grant agreement no. 309048

References

[1] M. Mokhtari, and F. Aminifar, “Toward wide-area oscillation control through doubly-fed induction generator wind farms,”*IEEE Transactions on Power Systems*, vol. 53, pp. 876–883, Nov. 2014.

[2] M. Mokhtari, J. Khazaei, and D. Nazarpour, “Sub-synchronous resonance damping via doubly fed induction generator,” *Electrical Power and Energy Systems*, vol. 29, pp. 2985 - 2992, Dec. 2013.

[3] R. Shah, N. Mithulananthan, and Kwang Y. Lee , “Large-Scale PV Plant With a Robust Controller Considering Power Oscillation Damping,” *IEEE Trans. Energy Conver.*, vol. 28, no. 1, pp. 106-116, Mar. 2013.

[4] R. Shah, N. Mithulananthan, and R.C.Bansal, “Oscillatory stability analysis with high penetrations of large-scale photovoltaic generation,” *Energy Conversion and Management,* vol. 65, pp. 420–429, Jan 2013.

[5] J. M. González-Caballín, E. Álvarez, A. J. Guttiérrez-Trashorras, A. Navarro-Manso, J. Fernández, E. Blanco, “Tidal current energy potential assessment by a two dimensional computational fluid dynamics model: The case of Avilés port (Spain),” *Energy Conversion and Management,* vol. 119, pp. 239-245, Jul. 2016.

[6] A. Vazquez, G. Iglesias, “A holistic method for selecting tidal stream energy hotspots under technical, economic and functional constraints” *Energy Conversion and Management*, vol. 117, pp. 420-430, Jun. 2016.

[7] J. Khan, C. Morton, and A. Rao, “Electrical power connectors for marine energy systems,” Tech. Rep. 20490-21-00 Rep-1, 2011, prepared by Powertech Labs Inc. for Natural Resources Canada (NRCan).

[8] K.R. Padiyar, V. Swayam, ‘‘ Prakash tuning and performance evaluation of damping controller for a STATCOM, *International Journal of Electrical Power & Energy Systems*, Vol. 25, no. 2, pp. 155–166. Feb. 2003.

[9] X. Xie, J. Xiao, C. Lu, and Y. Han, “Wide-area stability control for damping interarea oscillations of interconnected power systems,” *IET Gen. Tran. Dis*, vol. 153, pp. 507-514, Sept. 2006.

[10] M. Mokhtari, F. Aminifar, D. Nazarpour, and S. Golshannavaz, “Wide-area power oscillation damping with a Fuzzy controller compensating the continuous communication delays*”* *IEEE Trans. Power Syst.*, vol. 28, pp. 1997-2005, May 2013.

[11] N. R. Chaudhuri, S. Ray, R. Majumder, and B. Chaudhuri, “A new approach to continuous latency compensation with adaptive phasor power oscillation damping controller (POD),” *IEEE Trans. Power Syst.*, vol. 25, pp. 939–946, May 2010.

[12] W. Yao, L. Jiang, J. Y. Wen, and S. J. Cheng, “Delay-dependent stability analysis of the power system with a wide-area damping controller embedded,” *IEEE Trans. Power Syst.*, vol. 26, pp. 233–240, Feb. 2011.

[13] J. He, C. Lu, X.Wu, P. Li, and J. Wu, “Design and experiment of wide-area HVDC supplementary damping controller considering time delay in China southern power grid,” *IET Gen. Tran. Dist*, vol. 3, pp. 17–25, Jan. 2009.

[14] D. Dotta, A. S. Silva, and I. C. Decker, “Wide-area measurement-based two-level control design considering signals transmission delay,” *IEEE Trans. Power Syst.*, vol. 24, pp. 208–216, Feb. 2009.

[15] S. Wang, X. Meng, and T. Chen, “Wide-area control of power systems through delayed network communication,” *IEEE Trans Control Syst. Tech.*, vol. 20, pp. 495-503, Mar. 2012.

[16] S. E. B. Elghali, R. Balme, K. L. Saux, M. E. H. Benbouzid, J. F. Charpentier, and F. Hauville, “A simulation model for the evaluation of the electrical power potential harnessed by a marine current turbine,” *IEEE J. Ocean. Eng.*, vol. 32, no. 4, pp. 786–797, Oct. 2007.

[17] L. Myers, and A. S. Bahaj, “Simulated electrical power potential harnessed by marine current turbine arrays in the alderney race,” *Renewab. Energy*, vol. 30, no. 11, pp. 1713–1731, Sep. 2005.\

[18] L.Wang, and C.T. Hsiung, “Dynamic Stability Improvement of an Integrated Grid-Connected Offshore Wind Farm and Marine-Current Farm Using a STATCOM,”*IEEE Trans. Power Syst.*, vol. 26, no. 2, pp. 690–698, May. 2011.

[19] L.Wang, S.-S. Chen,W.-J. Lee, and Z. Chen, “Dynamic stability enhancement and power flow control of a hybrid wind and marine-current farm using SMES,” *IEEE Trans. Energy Convers*., vol. 24, no. 3, pp. 626–639, Sep. 2009.

[20] R.V. Rao, V.J.Savsani, and, D.P. Vakharia, “Teaching-learning-based optimization: An optimization method for continuous non-linear large scale problems,” *Information Sciences*, vol. 183, pp. 1-15, 2012.

[21] M. Crespinsek, S.H. Liu, and L. Mernik, “A note on teaching-learning-based optimization algorithm. Information Sciences,” *Information Sciences,* vol. 212, pp. 79-93, 2012.

[22] A. Baghlani, and M.H. Makiabadi, “Teaching-learning-based optimization algorithm for shape and size optimization of truss structures with dynamic frequency constraints” *IJST, Transactions of Civil Engineering*, Vol. 37, pp. 409-421, 2013.

[23] I. Kamwa, and R. Grondin, “PMU configuration for system dynamic performance measurement in large, multi-area power systems,” *IEEE Trans. Power Syst.,*vol. 17, pp. 385–394, May 2002.

[24] K. Mei, S. M. Rovnyak, and C.-M. Ong, “Clustering-based dynamic event location using wide-area phasor measurements,” *IEEE Trans. Power Syst.*, vol. 23, pp. 673–679, May 2008.

[25] P. Tripathy, S. C. Srivastava, and S. N. Singh, “A divide-by-difference-filter based algorithm for estimation of generator rotor angle utilizing synchrophasor measurements,” *IEEE Trans. Inst. and Meas.*, vol. 59, pp. 1562–1570, Jun. 2010.

[26] E. Ghahremani, and I. Kamwa, "Dynamic state estimation in power system by applying the extended Kalman filter with unknown inputs to phasor measurements," *IEEE Trans. Power Syst.*, vol. 26, pp. 2556–2566, Nov. 2011.

[27] P. Korba, R. Segundo, A. Paice, B. Berggren, and R. Majumder, "Time delay compensation in power system control," *European Union Patent,* EP08 156 785, May. 2008.

Appendix

Table A1
Pseudo code of TLBO

```
Set k=1 ;
Objective function f(X) , X=(x1, x2,....., xd)^T d=no. of design variables
Generate initial students of the classroom randomly X^i,1,2,..., nn=no. of students
Calculate objective function f(X) for whole students of the classroom
WHILE (the termination conditions are not met)
{ Teacher Phase }
Calculate the mean of each design variable X_Mean
Identify the best solution (teacher)
FOR i=1 → n
Calculate teaching factor T_F^i = round[1 + rand(0,1){2 − 1}]
Modify solution based on best solution(teacher)   X_new^i = X^i + rand(0,1).[X_teacher − (T_F^i . X_mean)]
Calculate objective function for new mapped student f(X_new^i)
IF X_new^i is better than X^i , i.e. f(X_new^i) < f(X^i)
                                X^i = X_new^i
END IF {End of Teacher Phase}
{ Student Phase}
Randomly select another learner X^j, such that j≠i
IF X^i is better than X^j, i.e f(X^i) < f(X^j)
                        X_new^i = X^i + rand(0,1).(X^i − X^j)
Else
                        X_new^i = X^i + rand(0,1).(X^j − X^i)
END IF
IF X_new^i is better than X^i, i.e f(X_new^i) < f(X^i)
                                X^i = X_new^i
END IF {End of Student Phase}
END FOR
Set k=k+1
END WHILE
Post process results and visualization
```

Table A.2
Parameters of Generators

	G_1	G_2	G_3	G_4	G_5	G_6
x_d	1.8	1.8	1.8	1.8	1.8	1.8
x'_d	3	3	3	3	3	3
x_q	1.7	1.7	1.7	1.7	1.7	1.7
T'_{do}	8	8	8	8	8	8
r_s	0.003	0.003	0.003	0.003	0.003	0.003
r_f	0.0006	0.0006	0.0006	0.0006	0.0006	0.0006
x_f	0.1	0.1	0.1	0.1	0.1	0.1
H	6.5	6.5	6.5	6.5	6.5	6.5

Table A.3
Parameters of Lines

Parameter	r	Xseries	Yshunt
Value	0.053 Ω/Km	0.53 Ω/Km	5.21 µs/Km

Table A.4
Parameters of single and aggregated DFIGs

Parameter	Single DFIG	Aggregated DFIGs
Rated power	1.5 MW	202.5 MW
Rated voltage	575 V	575 V
R_S	0.023 pu	0.023 pu
R'_r	0.016 pu	0.016 pu
L_{lS}	0.18 pu	0.18 pu
L'_{lr}	0.16 pu	0.16 pu
L_m	2.9 pu	2.9 pu
H_g	0.685 S	0.685 S
H_t	4.32 S	4.32 S
DC-link capacitor	10000 µf	135×10000 µf
DC-link voltage	1150 V	1150